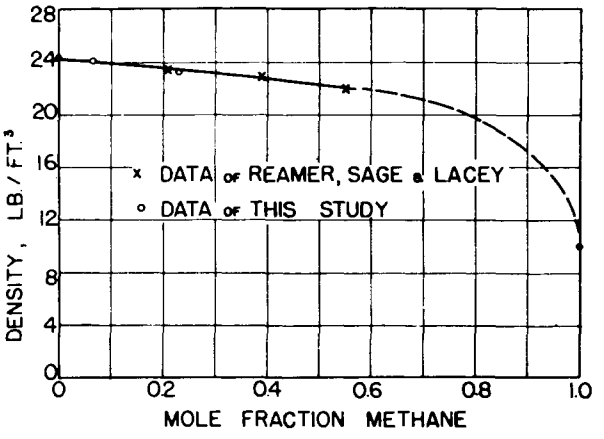


**Figure 9. Critical density**

It is necessary in order to explain this puzzling phenomenon to introduce the results of the rather extensive phase study made concurrently with the volumetric study on this system. It was discovered during this study that the methane–hydrogen sulfide system existed in two distinct liquid phases under certain pressure and temperature conditions. Kohn and Kurata (*3*) describe the phase behavior of this system. Ricci (*10*) also gives a discussion of the type of system involved here.

The bubble points observed by Reamer, Sage, and Lacey (*9*) at 30 and 40 mole % of hydrogen sulfide might be explained as a consequence of the manner in which they were determined. These investigators did not visually observe the bubble points. They were graphically calculated from the discontinuities in the isothermal volume-pressure derivatives. There are measurable discontinuities in the isothermal volume-pressure derivatives at the upper dew point line also.

In Figure 8, whereas the phase densities are indicated along the three-phase ($L_1$-$L_2$-$V$) line these densities leave something to be desired in the way of accuracy. The densities were calculated from isothermal compression lines and the small volumetric capacity of the equilibrium cell made the measurement of the incremental quantities of gas injected into the cell very difficult. The maximum error in the three-phase line densities is estimated at ±3% for the $L_1$ phase and ±10% for the $L_2$ and $V$ phases.

## CONCLUSION AND RECOMMENDATIONS

The volumetric data of this study are of sufficient accuracy for the design of equipment for the low temperature separation of hydrogen sulfide from methane. Because only two mixtures were studied which had bubble point curves, the bubble point density data are extremely meager. It would be desirable to supplement these data by additional low temperature data, especially on a mixture composed of approximately 50 mole % of hydrogen sulfide. It would be interesting, though of doubtful practical value, to obtain density data on the two-liquid phase region and along the critical solution line.


## ACKNOWLEDGMENT

Financial assistance during this study was received from the University of Kansas Fund for Research Project 17 and the Dow Chemical Co. All pure grade hydrocarbon liquids and gases used in this work were generously supplied by the Phillips Petroleum Co. Morris Teplitz, University of Kansas Research Foundation, generously loaned equipment and furnished many helpful suggestions.


## NOMENCLATURE

$P_c$ = critical pressure

$P_c'$ = pseudo-critical pressure, $\left(\sum_{i=1}^{n} N_i Pc_i\right)$

$Pr$ = pseudo-reduced pressure, $P/P_c'$

$T_c$ = critical temperature

$T_c'$ = pseudo-critical temperature, $\left(\sum_{i=1}^{n} N_i Tc_i\right)$

$Tr$ = pseudo-reduced temperature, $T/T_c'$

$Z$ = compressibility factor, $PV/RT$

$K$ = type $K$ singular point involving the critical identity of phases $L_2$ and $V$ in presence of phase $L_1$

$L_1$ = liquid phase having properties similar to pure liquid hydrogen sulfide at same temperature

$L_2$ = liquid phase having properties similar to pure liquid methane at same temperature

$V$ = vapor phase

## LITERATURE CITED


(1) Espach, R. H., *Ind. Eng. Chem.* **42**, 2235 (1950).
(2) Keyes, F. G., Burks, H. G., *J. Am. Chem. Soc.* **49**, 403 (1927).
(3) Kohn, J. P., Kurata, F., *A.I.Ch.E. Journal* **4**, No. 2, 211 (1958).
(4) Kohn, J. P., Kurata, F., *Petrol. Processing* **11**, No. 12, 57 (1956).
(5) Kvalnes, H. M., Gaddy, V. L., *J. Am. Chem. Soc.* **53**, 394 (1931).
(6) Michels, A., Nederbragt, G. W., *Physica* **3**, 569 (1936).
(7) Olds, R. H., Reamer, H. H., Sage, B. H., Lacey, W. N., *Ind. Eng. Chem.* **35**, 922 (1943).
(8) Reamer, H. H., Sage, B. H., Lacey, W. N., *Ibid.*, **34**, 1526 (1942).
(9) *Ibid.*, **43**, 976 (1951).
(19) Ricci, J. E., "The Phase Rule and Heterogeneous Equilibrium," Van Nostrand, New York, 1951.
(11) Standing, M. B., Katz, D. L., AIME Petroleum Technol. **146**, 140 (1942).
(12) West, J. R., *Chem. Eng. Progr.* **44**, 287 (1948).



Received for review April 8, 1957. Accepted August 25, 1958. Division of Industrial and Engineering Chemistry, 131st Meeting, ACS, Miami, Fla., April 1957.


# Thermal Conductivity of Fluids. Nitric Oxide


**G. NEAL RICHTER and B. H. SAGE**
**California Institute of Technology, Pasadena, Calif.**


Experimental determination of the thermal conductivity of nitric oxide in the gas phase is limited to measurements at atmospheric pressure. Johnston and Grilly (*7*) established the value of the thermal conductivity of nitric oxide at atmospheric pressure from –230° to 216° F. and Eucken (*2*) recorded values at –100° and 32° F. These data were obtained by use of hot wire cells of the potential lead type. Todd (*11*) measured the thermal conductivity of nitric oxide in equipment of parallel plate design. His reported experimental difficulties in the case of nitric oxide make the results uncertain. Winkelmann (*12*) was the first to measure the conductivity of nitric oxide, but because of the methods he employed the experimental results are primarily of historical interest.

Yost and Russell (*14*) summarized the properties of nitric oxide at atmospheric pressure; and the pressure-volume-

temperature relations and thermodynamic properties of nitric oxide are available (*3*, *9*). Experimental data concerning the thermal properties and viscosity of nitric oxide are summarized in an article by Hilsenrath and Touloukian (*5*) and in two publications of the National Bureau of Standards (*4*, *13*).

## METHODS AND EQUIPMENT

The equipment used for the present study consisted in principle of two concentric spherical shells whose temperatures were measured while a known radial thermal flux passed between them. Figure 1 shows the apparatus in

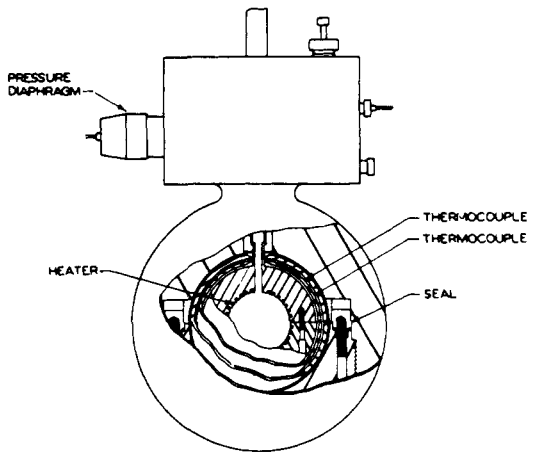


**Figure 1. Schematic diagram of thermal conductivity cell**

schematic diagram. The shells, supported by small needle-like pins, surrounded an inner sphere within which was placed an electric heater. The whole assembly was surrounded by an outer spherical pressure vessel and immersed in an agitated liquid bath.

The amount of energy added to the inner sphere was determined by conventional calorimetric means involving the potential lead technique. The uncertainty in the measurement of the energy added to the inner sphere was less than 0.05%. The temperature of the agitated liquid bath surrounding the thermal conductivity cell was determined with a resistance thermometer of the strain-free type (*8*). The bath temperature was controlled by a resistance thermometer through a photoelectric modulating circuit, and deviations of temperature of more than 0.01° F. at any one point with respect to time were infrequent. The temperature of the surface of the two spherical shells was determined with platinum, platinum-iridium thermocouples mounted to record the temperature of the outer surface of the inner shell and the inner surface of the outer shell. A detailed description of the equipment is available (*10*).

## ANALYSIS

In accordance with methods of analysis employed earlier (*10*), the thermal conductivity was related to the electrical energy addition and certain correction factors as:

$$k = \left(\frac{\mathring{q}_m (r_0 - r_i)\phi_A}{4\pi r_0 r_i (t_i - t_0)}\right) - (\mathring{q}_p + \mathring{q}_r + \mathring{q}_s)\left(\frac{(r_0 - r_i)\phi_A}{4\pi r_0 r_i (t_i - t_0)}\right) \quad (1)$$

It follows from the conservation of energy that:

$$\mathring{Q} = EI = \mathring{q}_c + \mathring{q}_p + \mathring{q}_r + \mathring{q}_s \quad (2)$$

In order to evaluate the thermal conductivity at zero thermal flux, it was necessary to correct the measured thermal flux for conduction through the pins supporting the shells, radiant transfer between the shells, and thermal transfer through the stem. These corrections are identified in Equations 1 and 2 as $\mathring{q}_p$, $\mathring{q}_r$, and $\mathring{q}_s$, respectively. The thermal transfer through the pins of the spheres was expressed in terms of an equivalent thermal conductivity:

$$k_p = \frac{\left[\frac{24\pi k_{ss} r_p^2 (t_i - t_0)}{5(r_0 - r_i)}\right](r_0 - r_i)\phi_A}{4\pi r_0 r_i (t_i - t_0)} \quad (3)$$

Similarly, following the Stefan-Boltzmann law, the radiant transfer was expressed in terms of the coefficient:

$$k_r = \frac{\phi(r_i r_0)\,\phi(\epsilon)\left(\frac{t_i^3 + t_0^3}{2}\right)(t_i - t_0)}{(t_i - t_0)} \quad (4)$$

It has been found that with a properly adjusted guard heater thermal transfer through the stem is negligible. For this reason it was neglected.

It is evident that the correction terms both for conduction through the pins and for radiation approach a finite value as the flux is reduced without limit. Therefore, thermal conductivity was evaluated from the apparent thermal conductivity established from

$$k_m = \frac{\mathring{q}_m (r_0 - r_i)\phi_A}{4\pi r_i r_0 (t_i - t_0)} \quad (5)$$

in the following way:

$$k = k_m - k_r - k_p - k_s \quad (6)$$

Values of the transfer by conduction through the pins and by radiation were determined with the thermal conductivity apparatus evacuated to a pressure less than 1 micron. Measurements at a series of different rates of energy addition and at different temperatures permitted evaluation of $k_p$ and $k_r$ by the simultaneous solution of Equations 3 and 4. These values are recorded in Table I. The corrections

**Table I. Coefficients of Thermal Transport by Conduction through the Pins and by Radiation**

| Temp., °F. | Coefficient of Thermal Transport, B.t.u./(Hr.) (Ft.) (°F.) | |
|---|---|---|
| | Conduction[a] | Radiation |
| 40 | $3.14 \times 10^{-4}$ | $4.74 \times 10^{-4}$ |
| 100 | 3.24 | 6.66 |
| 160 | 3.33 | 9.04 |
| 220 | 3.43 | 11.92 |
| 280 | 3.53 | 15.35 |
| 340 | 3.63 | 19.39 |
| 400 | 3.73 | 24.08 |

[a]Conduction through pins.

upon the measurements of thermal conductivity amount to approximately 3% at 40°F. and nearly 15% at 400° F. It was assumed that the corrections were a function of temperature only and not a function of pressure. The absorption of radiation by the nitric oxide was neglected. As a result of some earlier difficulties with drift in the calibration of the thermocouples used to measure the temperature of the concentric shells, data were obtained for helium. The thermocouple calibrations were found to be stable during this investigation. Values of thermal conductivity for helium at atmospheric pressure of 0.08843 and 0.09911 B.t.u./(hr.) (ft.) (°F.) at 100° and 220°F. were obtained with the calibration of the thermocouples employed. These values compare with 0.08854 and 0.09946 B.t.u./(hr.) (ft.) (°F.) reported by Hilsenrath and Touloukian (*5*) for helium at the same states. The agreement was within the experimental uncertainty of measurement.

## MATERIALS

The nitric oxide, obtained from the Matheson Co., Inc., was reported to contain less than 0.02 weight fraction of

impurities. The gas was treated with potassium hydroxide and dried in accordance with the purification procedure of Johnston and Giauque (6), after which it was stored in a stainless steel cylinder until ready for use. This purification system has been found to give a product containing less than 0.002 weight fraction of impurities as determined by measurements of the specific weight of gas at atmospheric pressure.

## EXPERIMENTAL RESULTS

The experimental results obtained for nitric oxide in the gas phase are recorded in Table II. The state, temperature difference, and apparent thermal conductivity are recorded for each set of measurements. Extrapolated values of apparent thermal conductivity corresponding to a zero temperature difference between the shells are included, as well as corrections for conduction through the pins and for radiation, and the final value of thermal conductivity. Values of apparent thermal conductivity were calculated directly from measurements of the energy addition and the temperature difference between the spheres, as indicated in Equation 5. At the higher rates of energy addition, differences of as much as 2% between the apparent thermal conductivity as established from the upper hemisphere and from the lower hemisphere occurred. However, the mean value of apparent thermal conductivity was used to evaluate the thermal conductivity recorded in Table II.

Table III gives the results obtained from smoothing the values of thermal conductivity recorded in Table II with respect to temperature and pressure. The results do not involve probable errors greater than 4%. However, the quantity of experimental data was not sufficient to permit meaningful statistical analysis of the several uncertainties involved in this experimental study.

Figure 2 presents experimental data of Table II for the thermal conductivity of nitric oxide at atmospheric pressure as a function of temperature, and includes measurements of Johnston and Grilly (7) and Eucken (2). The latter sets of

**Table II. Experimental Results**

| Nominal Temp., °F. | Pressure, P.S.I.A. | Temp. Difference[a], °F. | Apparent Thermal Conductivity[a], B.t.u./(Hr.) (Ft.) (°F.) | Correction, B.t.u./(Hr.) (Ft.) (°F.) | | Thermal Conductivity, B.t.u./(Hr.) (Ft.) (°F.) |
|---|---|---|---|---|---|---|
| | | | | Conduction[b] | Radiation | |
| 40 | 15.1 | 1.106 | 0.01278 | | | |
| | | 2.398 | 0.01284 | | | |
| | | 4.830 | 0.01290 | | | |
| | | 0.000 | 0.01276 | $3.14 \times 10^{-4}$ | $4.74 \times 10^{-4}$ | 0.01197 |
| | 577.4 | 0.938 | 0.01454 | | | |
| | | 1.622 | 0.01463 | | | |
| | | 2.418 | 0.01466 | | | |
| | | 0.000 | 0.01456 | 3.14 | 4.74 | 0.01377 |
| | 972 | 0.944 | 0.01648 | | | |
| | | 1.525 | 0.01675 | | | |
| | | 1.908 | 0.01871 | | | |
| | | 0.000 | 0.01607 | 3.14 | 4.74 | 0.01528 |
| 100 | 15.4 | 0.598 | 0.01444 | | | |
| | | 1.252 | 0.01437 | | | |
| | | 2.200 | 0.01446 | | | |
| | | 0.000 | 0.01439 | 3.24 | 6.66 | 0.01340 |
| 160 | 15.2 | 0.712 | 0.01580 | | | |
| | | 1.346 | 0.01599 | | | |
| | | 2.065 | 0.01577 | | | |
| | | 0.000 | 0.01585 | 3.33 | 9.04 | 0.01461 |
| 220 | 15.3 | 0.642 | 0.01723 | | | |
| | | 1.272 | 0.01705 | | | |
| | | 1.972 | 0.01732 | | | |
| | | 0.000 | 0.01712 | 3.43 | 11.92 | 0.01558 |
| | 809 | 0.652 | 0.01936 | | | |
| | | 1.172 | 0.01946 | | | |
| | | 1.688 | 0.01962 | | | |
| | | 0.000 | 0.01918 | 3.43 | 11.92 | 0.01764 |
| | 1391 | 0.738 | 0.02082 | | | |
| | | 1.238 | 0.02096 | | | |
| | | 1.773 | 0.02140 | | | |
| | | 0.000 | 0.02089 | 3.43 | 11.92 | 0.01936 |
| 280 | 15.2 | 0.686 | 0.01887 | | | |
| | | 1.131 | 0.01882 | | | |
| | | 1.999 | 0.01897 | | | |
| | | 0.000 | 0.01879 | 3.53 | 15.35 | 0.01690 |
| 340 | 15.4 | 0.683 | 0.02010 | | | |
| | | 1.160 | 0.02042 | | | |
| | | 1.828 | 0.02042 | | | |
| | | 0.000 | 0.01997 | 3.63 | 19.39 | 0.01767 |
| | 950 | 0.570 | 0.02286 | | | |
| | | 0.955 | 0.02300 | | | |
| | | 1.680 | 0.02324 | | | |
| | | 0.000 | 0.02274 | 3.63 | 19.39 | 0.02044 |
| 400 | 15.2 | 0.644 | 0.02232 | | | |
| | | 1.066 | 0.02212 | | | |
| | | 1.660 | 0.02218 | | | |
| | | 0.000 | 0.02212 | 3.73 | 24.08 | 0.01934 |

[a]These values represent average temperature difference and associated average thermal conductivity for the upper and lower hemispheres.
[b]Conduction through pins.

Table III. Thermal Conductivity of Nitric Oxide

| Pressure, P.S.I.A. | 40° F. | 100° F.[a] | 160° F.[a] | 220° F. | 280° F.[a] | 340° F. | 400° F.[a] |
|---|---|---|---|---|---|---|---|
| 14.696 | 0.01209[b] | 0.01329 | 0.01448 | 0.01566 | 0.01682 | 0.01799 | 0.01917 |
| 50 | 0.01220 | 0.01339 | 0.01457 | 0.01575 | 0.01691 | 0.01808 | 0.01926 |
| 100 | 0.01236 | 0.01353 | 0.01470 | 0.01588 | 0.01705 | 0.01821 | 0.01938 |
| 150 | 0.01251 | 0.01367 | 0.01483 | 0.01601 | 0.01717 | 0.01834 | 0.01951 |
| 200 | 0.01267 | 0.01381 | 0.01497 | 0.01614 | 0.01729 | 0.01847 | 0.01963 |
| 400 | 0.01329 | 0.01438 | 0.01550 | 0.01665 | 0.01781 | 0.01898 | 0.02015 |
| 600 | 0.01391 | 0.01495 | 0.01602 | 0.01717 | 0.01832 | 0.01949 | 0.02067 |
| 800 | 0.01454 | 0.01550 | 0.01656 | 0.01769 | 0.01884 | 0.02001 | 0.02118 |
| 1000 | 0.01516 | 0.01606 | 0.01708 | 0.01820 | 0.01936 | 0.02052 | 0.02170 |
| 1250 | 0.01594[c] | 0.01677 | 0.01775 | 0.01884[c] | 0.02000 | 0.02116[c] | 0.02234 |
| 1500 | 0.01671[c] | 0.01748 | 0.01842 | 0.01949[c] | 0.02065 | 0.02118[c] | 0.02298 |

[a] Values of thermal conductivity are interpolated.
[b] Thermal conductivity expressed in B.t.u./(hr.) (ft.) (° F.).
[c] Values are extrapolated.

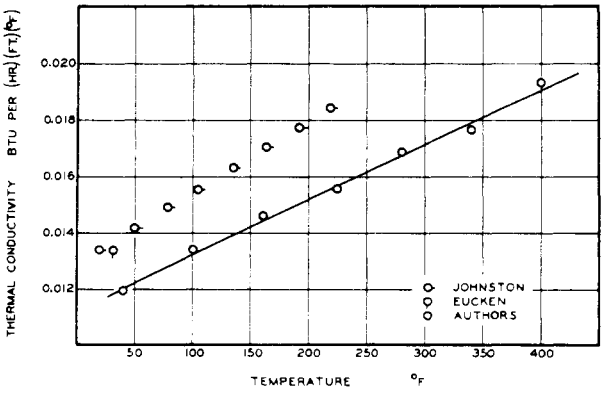


Figure 2. Thermal conductivity of nitric oxide at atmospheric pressure

measurements were both made using the conventional heated-wire potential-lead technique, and the disagreement between these data and the data of the present investigation is somewhat greater than would be expected from a consideration of the experimental uncertainties. Further experimental work will be required to resolve this discrepancy.

Figure 3 depicts the influence of pressure upon the thermal conductivity of nitric oxide at temperatures from 40° to 400° F. The data indicate a somewhat larger change in the conductivity with pressure than would be expected from the predictions of Comings and Nathan (*1*).

It was planned originally to carry this experimental investigation to a pressure of 5000 p.s.i. However, significant decomposition of the nitric oxide occurred at pressures above 2000 p.s.i. at 40° F., and at pressures of the order of 1000 p.s.i. at 340° F. Investigation of the composition of the fluid remaining after such noticeable decomposition indicated that the reaction was of the following nature:

$$4\,NO \rightleftarrows 2\,NO_2 + N_2 \qquad (7)$$

The chemical potentials of the components indicate that equilibrium should be expected from the system when it is composed predominantly of nitrogen and nitrogen dioxide (*14*). Decompositions such as described were not encountered in earlier studies of the pressure-volume-temperature relations of nitric oxide (*3*) and do not appear to be reported elsewhere. For this reason it is the authors' belief that the decomposition was prompted by catalytic action of the platinum associated with the thermocouples or of the chrome finish upon the interior of the outer pressure vessel. The rate of change of pressure within the thermal conductivity cell under isothermal-isochoric conditions is shown in Table IV. It is apparent that a rapid increase in the rate of change of pressure was encountered with an increase in pressure or an increase in temperature. Investigation of

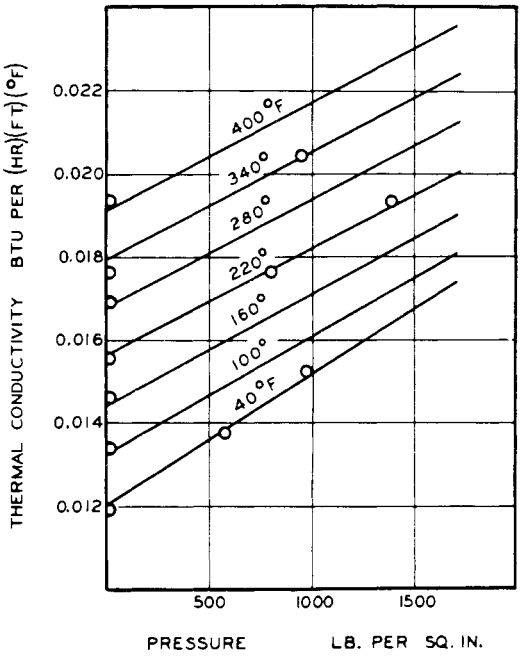


Figure 3. Effect of pressure on thermal conductivity of nitric oxide

the decomposition of the nitric oxide was not carried further, because it was outside the primary purpose of the study.


## ACKNOWLEDGMENT

H. H. Reamer assisted with the laboratory program.


## NOMENCLATURE

$E$ = electromotive force drop through heater, volt
$Q$ = total energy flux, B.t.u. per hour
$I$ = current through heater, ampere
$k$ = thermal conductivity, B.t.u./(hr.) (ft.) (° F.)
$k_m$ = coefficient of measured thermal transport, B.t.u./(hr.) (ft.) (° F.)
$k_p$ = coefficient of thermal transport through pins, B.t.u./(hr.) (ft.) (° F.)

Table IV. Observed Rates of Decomposition of Nitric Oxide

| Temp., ° F. | Pressure, P.S.I.A. | Rate of Change of Pressure, (Lb./Sq.In.)/(Hr.) |
|---|---|---|
| 40 | 972 | Not measurable |
| | 4800 | 130 |
| 220 | 809 | 0.10 |
| | 1391 | 0.94 |
| 340 | 950 | 0.55 |
| | 1655 | 6.0 |

$k_r$ = coefficient of thermal transport by radiation, B.t.u./(hr.) (ft.) (°F.)
$k_s$ = coefficient of thermal transport through stem, B.t.u./(hr.) (ft.) (°F.)
$k_{st}$ = thermal conductivity of steel, B.t.u./(hr.) (ft.) (°F.)
$\dot{q}_c$ = rate of heat transfer by conduction through the fluid, B.t.u. per hour
$\dot{q}_m$ = measured rate of energy addition, B.t.u. per hour
$\dot{q}_p$ = rate of heat transfer through pins, B.t.u. per hour
$\dot{q}_r$ = rate of heat transfer by radiation, B.t.u. per hour
$\dot{q}_s$ = rate of heat transfer through stem, B.t.u. per hour
$r_i$ = inner radius, feet
$r_o$ = outer radius, feet
$r_p$ = radius of pins, feet
$t_i$ = temperature at inner radius, °F.
$t_o$ = temperature at outer radius, °F.
$\epsilon$ = emissivity
$\phi$ ( ) = function of
$\phi A$ = ratio of area of complete sphere to area of sphere minus area intercepted by shaft

## LITERATURE CITED


(1) Comings, E. W., Nathan, M. F., *Ind. Eng. Chem.* **39**, 964 (1947).
(2) Eucken, A., *Physik Z.* **14**, 324 (1913).
(3) Golding, B. H., Sage, B. H., *Ind. Eng. Chem.* **43**, 160 (1951).
(4) Hilsenrath, J. and others, "Tables of Thermal Properties of Gases," Natl. Bur. Standards, Circ. **564** (1955).
(5) Hilsenrath, J., Touloukian, Y. S., *Trans. Am. Soc. Mech. Engrs.* **76**, 967 (1954).
(6) Johnston, H. L., Giauque, W. F., *J. Am. Chem. Soc.* **51**, 3194 (1929).
(7) Johnston, H. L., Grilly, E. R., *J. Chem. Phys.* **14**, 233 (1946).
(8) Meyers, C. H., *Bur. Standards J. Research* **9**, 807 (1932).
(9) Opfell, J. B., Schlinger, W. G., Sage, B. H., *Ind. Eng. Chem.* **46**, 189 (1954).
(10) Richter, G. N., Sage, B. H., *Ind. Eng. Chem., Chem. Eng. Data Ser.* **2**, No. 1, 61 (1957).
(11) Todd, G. W., *Proc. Roy. Soc. (London)* **A 83**, 19 (1909).
(12) Winkelmann, A., *Ann. phys.* **156**, 497 (1875).
(13) Wooley, H. W., "Thermodynamic Properties of Gaseous Nitric Oxide," Natl. Bur. Standards, Rept. **2602** (1955).
(14) Yost, D. M., Russell, H., Jr., "Systematic Inorganic Chemistry," Chap. I, Prentice-Hall, New York, 1944.



Received for review November 14, 1957. Accepted June 2, 1958. Work sponsored by Project SQUID which is supported by the Office of Naval Research under Contract N6-ori-105, T. O. III, NR-098-038. Reproduction in full or in part is permitted for any use of the United States Government.


# Low Temperature Vapor-Liquid Equilibrium in Light Hydrocarbon Mixtures: Methane-Ethane-Propane System


**A. ROY PRICE[1] and RIKI KOBAYASHI**
**The Rice Institute, Houston, Tex.**


While the vapor-liquid equilibrium data for light hydrocarbons are relatively abundant above 50° F., a review of the literature indicates a need for such data at lower temperatures and high pressures. Very few phase equilibria data are available with which to test correlations extending into the low temperature regions. The systems which have been studied heretofore (and their references) are listed below:

| System | Source |
|---|---|
| Methane-ethylene | (*9, 34*) |
| Methane-ethane | (*3, 14, 25*) |
| Methane-propane | (*1, 27*) |
| Methane-n-butane | (*18, 28*) |
| Ethylene-ethane | (*13, 15*) |
| Ethylene-propane | (*16, 26*) |
| Ethylene-propylene | (*16*) |
| Methane-ethylene-ethane | (*9*) |
| Ethylene-ethane-acetylene | (*15*) |
| Natural gases | (*6, 7, 31*) |

The purpose of this investigation was to obtain phase equilibria data at low temperatures to supplement the data above and provide a basis for the evaluation of correlations for low temperature $K$-values. The ternary methane-ethane-propane system was selected because of its basic, yet multicomponent nature. Six temperatures were investigated, extending from 50° down to −200° F. Pressures at 100 and 200 p.s.i. intervals up to the critical states were chosen.

## EXPERIMENTAL APPARATUS

The vapor recycle equipment used by Harvey (*10*) was modified for this study. The apparatus can be divided into six functional sections: equilibrium, pressure control, temperature control, charge, sampling, and vacuum systems.

[1]Present address, Humble Oil and Refining Co., Baytown, Tex.

Figure 1 presents the assembly diagram of the experimental apparatus.

The equilibrium cell, $C$, is submerged in a constant temperature bath contained in a Dewar flask. A Jerguson transparent gage with stainless steel body was used for the cell. Inlet and outlet holes were drilled in the bottom and top, respectively. Thermocouple wells of capillary steel tubing were inserted about an inch from the top and bottom, and a liquid sample tap was drilled near the bottom. Teflon gaskets were used between the glass windows and the metal body, and have been successful down to −250° F. at pressures up to 2000 p.s.i. The windows of the equilibrium cell were centered with respect to the slits in the Dewar flask to permit clear visibility of the cell contents at all times.

Another Jerguson transparent gage, $R$, was located outside the bath to permit detection of any retrograde condensation of the recycle vapors at room temperature. A totally enclosed magnetic pump, $P$, provided the recirculation without introducing a source of high pressure leaks. The variable volume cell, $V$, served as a reservoir of vapor and also as a mercury receptacle used in the regulation of pressure during the charging, equilibration, and liquid sampling periods.

The primary cooling system was similar to that used by Bloomer and others in their study of the methane-ethane system (*3*). The temperature regulation was provided by controlling the rate of evaporation of liquid nitrogen. In this manner, temperature could be regulated to within 0.1° F. of a preassigned value. Calibrated copper-constantan thermocouples placed in the two thermowells and at three locations within the liquid bath indicated the temperature.

The various ternary mixtures studied were synthesized within the equilibrium cell by a trial and error procedure of adding each pure component into the cell. The last traces of heavy hydrocarbons, water, and carbon dioxide were